



WICHITA STATE
UNIVERSITY

UNIVERSITY LIBRARIES

Photopolymerization kinetics of UV-curable polyester powder coatings containing urethane methacrylate reactive diluents

Item Type	Article
Authors	Hammer, Theodore J.;Pugh, Coleen;Soucek, Mark D.
Citation	Hammer, T.J., Pugh, C. & Soucek, M.D. Photopolymerization kinetics of UV-curable polyester powder coatings containing urethane methacrylate reactive diluents. J Coat Technol Res (2025). https://doi.org/10.1007/s11998-025-01079-7
DOI	10.1007/s11998-025-01079-7
Publisher	Springer
Download date	2026-05-20 03:50:41
Link to Item	https://hdl.handle.net/10057/29794



Photopolymerization kinetics of UV-curable polyester powder coatings containing urethane methacrylate reactive diluents

Theodore J. Hammer , Coleen Pugh, Mark D. Soucek

Received: 28 October 2024 / Revised: 10 January 2025 / Accepted: 15 January 2025
© The Author(s) 2025

Abstract A series of small molecule urethane methacrylates were synthesized and used as reactive diluents for UV-curable polyester powder coatings. A UV-curable polyester oligomer was prepared and formulated with the reactive diluents and a photoinitiator package. Kinetics studies were carried out using photo-differential scanning calorimetry (photo-DSC). The influence that the reactive diluent concentration, UV-light intensity, temperature, and atmosphere had on the reaction kinetics was investigated. Crosslinked samples that were analyzed via DSC showed that the glass transition temperature correlated well with the extent of conversion. In general, lower curing temperatures (i.e., $\leq 80^\circ\text{C}$) significantly reduced the conversion and polymerization rate. However, the use of a mono-functional reactive diluent facilitated much higher conversions than the UV-curable polyester control, even at just 5 wt% loading level. These findings suggest that reactive diluents can be used to improve the low temperature cure capability of UV-curable polyester powder coatings.

Keywords UV-curing, Powder coating, Photopolymerization kinetics, Methacrylate-terminated polyester, Photo-DSC

Introduction

Thermoset powder coatings are one of the fastest growing coating technologies due to their excellent durability, weatherability, and mechanical properties.^{1–3} Powder coatings also offer the unique advantage in that they emit little to no volatile organic compounds (VOCs). As such, powder coatings are inherently less hazardous to both the user and the environment when compared to liquid coating systems.^{4–6} However, despite the numerous advantages that thermoset powder coatings have, there are also several disadvantages as well. Thermally-cured powder coatings usually require harsh curing conditions, i.e., $160\text{--}200^\circ\text{C}$ for anywhere from 10–30 min. This prohibits many powder coating systems from being applied to heat sensitive substrates such as wood, plastic, composites, or pre-assembled components. Furthermore, because the film formation and curing processes occur concomitantly, thermally-cured powder coatings frequently exhibit orange peel defects. These defects are aesthetically displeasing and, in severe cases, can be detrimental to the performance of the coating. To overcome some of these limitations, UV-curable powder coatings were introduced.⁷

Like thermally-cured powder coatings, UV-curable powder coatings require a preliminary heating step so that the powder particles can melt and coalesce into a uniform film. The initial film formation step can be accomplished in a few minutes using either IR or convection heating.⁸ Temperatures between 90 and 120°C , which is typically the T_g of the resin + 50°C , are most common. Good flow and leveling can be achieved because the viscosity does not increase during the film formation step like it does with thermally-cured systems. Once a uniform film has been obtained, the molten sample is exposed to UV-light to instantaneously generate a crosslinked film. Despite the benefits with UV-curing technology, the proper for-

T. J. Hammer, C. Pugh, M. D. Soucek (✉)
School of Polymer Science and Polymer Engineering,
University of Akron, Akron, OH 44325, USA
e-mail: msoucek@uakron.edu

C. Pugh
Department of Chemistry and Biochemistry, Wichita State
University, Wichita, KS 67260, USA

mulation of a UV-curable coating can be a challenge. Photopolymerization reactions are highly complex and are affected by several variables such as the curing temperature, the UV-light intensity, the photoinitiator type, the photoinitiator concentration, the presence or absence of pigment, and whether or not the reaction is conducted in the presence of an inert atmosphere.^{9–13} As such, a thorough understanding of the photopolymerization kinetics is essential when designing a UV-curable coatings formulation.

Several investigations have explored the photopolymerization kinetics of UV-curable powder coatings. Castell et al. used real-time Fourier transform infrared (FTIR) spectroscopy, photo-DSC, and photo-rheology experiments to study the kinetics of a commercially available methacrylated polyester powder coating system.¹⁴ Conversions generally ranged between 50–75%, depending on the curing temperature, the type of photoinitiator that was used, and the photoinitiator loading level. The optimum photoinitiator package consisted of a 1:1 blend (2.5 wt% of the entire formulation) of phenylbis(2,4,6-trimethylbenzoyl)phosphine oxide (Irgacure 819) and 1-[4-(2-hydroxyethoxy)-phenyl]-2-hydroxy-2-methyl-1-propane-1-one (Irgacure 2959). Shi et al. developed semi-crystalline hyperbranched poly(ester-amide)s and semi-crystalline dendritic poly(ether-amide)s with acrylate functional groups for UV-curable powder coating applications.^{15,16} Photo-DSC experiments found that conversions between 60–70% could be obtained when 4 wt% of 1-hydroxycyclohexyl phenyl ketone (Irgacure 184) was used as the photoinitiator. Maurin et al. used real-time FTIR spectroscopy to evaluate how several liquid acrylate monomers having a functionality of 2, 3, or 4, affected the kinetics of two different UV-curable powder coating resins.¹⁷ The di- and tri-functional monomers generally increased the degree of conversion whereas the tetra-functional monomer decreased the degree of conversion due to premature vitrification of the polymer network. The same research group also studied the termination behavior of a UV-curable powder coating formulation using real-time FTIR spectroscopy.¹⁸ The photoinitiator concentration, the formulation viscosity, and the degree of conversion had an influence on the mechanism of termination, i.e., either bimolecular termination or monomolecular termination.

In a previous study, the relationship between the crosslinked network structure and the thermo-mechanical properties of UV-curable polyester powder coatings containing urethane methacrylate reactive diluents was evaluated.¹⁹ Here, the photopolymerization kinetics of those same formulations were studied to understand how the number of methacrylate groups and the chain length of the reactive diluent affected the conversion and polymerization rate. Several variables such as the curing temperature, curing atmosphere, and the UV-light intensity were adjusted to understand their effects on the reaction kinetics. The T_g s of the

crosslinked formulations were subsequently determined and related to the degree of conversion.

Experimental

Materials

All reagents and solvents were used as received, without further purification, unless otherwise noted. Benzoin (98%), 4-dimethylaminopyridine (DMAP; 99%), dibutyltin (IV) oxide (DBTO; > 98%) ethylene carbonate (EC; 98%), ethylenediamine (EDA; 99%), 1,6-hexanediamine (HDA; 98%), hydroquinone (99%), methacrylic anhydride (MAAn; 94%), terephthalic acid (TPA; 98%), and triethylamine (TEA; 99%) were obtained from Sigma Aldrich. Dodecylamine (DDA; 98.50%) and neopentyl glycol (NPG; 99%) were obtained from Alfa Aesar. Dichloromethane (DCM; 99.9%), dimethylformamide (DMF; ≥ 99.8%), and tetrahydrofuran (THF; > 99%) were obtained from Fisher Scientific. Irgacure 184 (1-hydroxycyclohexyl phenyl ketone) and Irgacure 819 (phenylbis-(2,4,6-trimethylbenzoyl)phosphine oxide) were obtained from BASF. Modaflow 6000 was kindly supplied by Allnex. DMAP was recrystallized from ethyl acetate prior to use.

Techniques and instrumentation

Reactions were conducted under an atmosphere of N_2 using standard Schlenk line techniques unless otherwise noted. All 1H NMR spectra (δ , ppm) were recorded on a Varian Mercury 300 MHz NMR spectrometer using $CDCl_3$ or D_2O as solvent. Fourier transform infrared (FTIR) spectroscopy was recorded on a Nicolet iS50 spectrometer using an attenuated total reflection (ATR) diamond attachment. A total of 16 scans at 4 cm^{-1} resolution were recorded for each sample. All spectra were analyzed using OMNIC software. Number average molecular weight (M_n) and polydispersity (PDI; $PDI = M_w/M_n$) were measured with an HLC-8320 GPC from Tosoh equipped with a refractive index detector. The samples were analyzed with Styragel HT2, HR1, HR0.5, and 500 Å Ultra-styragel columns and compared against a polystyrene (GPC_{PSI}) standard. THF was used as the eluent at a flow rate of 1.0 mL/min. Samples were prepared at concentration of 3.0 mg/mL. Prior to injection, samples were filtered using a 0.45 μm syringe filter. Differential scanning calorimetry (DSC) experiments were conducted on a TA Instruments model Q2000 using aluminum hermetic pans. After the samples were cured, heat/cool/heat cycles were conducted between 0 and 200°C with a 20°C heating rate. The glass transition temperature (T_g) was taken as the middle of the inflection point on the second heating cycle. All samples were run in duplicate.

Photopolymerization kinetic studies

All photo-DSC experiments were conducted on a TA Instruments model Q2000 equipped with a Novacure UV-light source (model N2001-A1; Hg bulb). All samples were approximately (but precisely weighed and recorded) 3.00 mg to minimize the influence of sample thickness on the reaction kinetics. All experiments used the same blank aluminum hermetic pan for consistency. Experiments were conducted using the following procedure (Fig. 1): Samples were first heated to the temperature of interest, e.g., 100°C, and allowed to equilibrate. Once the temperature had equilibrated, data collection was started. A 150 s hold period, with no UV-light exposure, was used to establish the baseline. Following this dark period, the UV-light shutter was opened, and the sample was exposed to UV light for 5 min. The shutter was subsequently closed and then another 150 s hold period, with no UV-light exposure, was used to re-establish the baseline. A minimum of three replicates were performed for each photo-DSC experiment. Sigmoidal integrations were used to account for any deviations in the baseline. The air flow (either nitrogen or breathing air) was regulated at 40 mL/min. Light intensity was adjusted using neutral density light filters (10% and 1%). The intensity of the UV-light was analyzed with a UV-power puck, i.e., either 12 or 1.2 mW/cm². The calculations that were used to determine percent conversion were made using the enthalpy of reaction for a methacrylate double bond ($\Delta H = 54.8$ kJ/mol).^{20,21}

Equations (1) and (2) below were used to determine the degree of conversion.^{22,23} Equation (1) was used to calculate the theoretical enthalpy value (ΔH_{theory}) for complete reaction of the methacrylate double bonds where f is the degree of functionality (e.g., two for two methacrylate groups per oligomer), N is the weight fraction of the methacrylate component, the enthalpy associated with the complete reaction of a methacrylate double bond ($\Delta H_{methacrylate}$) is equal to 54.8 kJ/mol (54,800 J/mol), and MW is the molecular weight (g/mol) of the particular methacrylate component. The molecular weight of the methacrylated polyester (MPE) was obtained from ¹H NMR spectroscopy via end group analysis. The molecular weights of each reactive diluent were based on the theoretical molecular weight for a pure compound. Equation (2) uses the experimental reaction enthalpy (ΔH_{actual}) that was captured in the photo-DSC experiment. Dividing the experimental enthalpy value by the theoretical enthalpy value and then multiplying by 100 gave the conversion as a percentage.

$$\Delta H_{theory} \left(\frac{J}{g} \right) = \left(\frac{f_1 N_1 \Delta H_{methacrylate}}{MW_1} + \frac{f_2 N_2 \Delta H_{methacrylate}}{MW_2} \right) \quad (1)$$

$$Conversion(C) = \frac{\Delta H_{actual}}{\Delta H_{theory}} * 100 \quad (2)$$

Synthetic methods

The full synthetic procedures for the polyester oligomers and for the urethane methacrylate reactive diluents is provided in a separate study.¹⁹ The characterization details are enclosed below. Figure 2 below provides the chemical structures of the methacrylated polyester oligomer and the three reactive diluents.

Synthesis of hydroxyl-terminated polyester

A clear and colorless glassy solid was obtained (409.42 g, 93.73% yield). $M_{n,NMR} = 2.37 \times 10^3$; $GPC_{PSt} M_n = 2.08 \times 10^3$, PDI = 1.80; $T_g = 59^\circ C$ (2nd heating scan, 20°C /min); TAN = 1.54 mg KOH/g resin. δ (ppm): 1.01 (–CH₃), 1.17 (–CH₃), 3.40 (–CH₂OH), 4.20–4.26 (–CO–O–CH₂–), 7.66 (ArH), 8.08 (ArH). FTIR (ATR): 3500, 1714, 1473, 1262, 1243, 1097, 1016, 725 cm^{–1}.

Synthesis of methacrylated polyester (MPE)

A white powdery solid was obtained (458.61 g, 90.15% yield). $M_{n,NMR} = 3.63 \times 10^3$; $GPC_{PSt} M_n = 2.27 \times 10^3$, PDI = 1.65 (post precipitation mass and PDI); $T_g = 47^\circ C$ (2nd heating scan, 20°C /min). δ (ppm): 1.10–1.17 (–CH₃), 1.94 (–CH₃, methacrylate), 4.06–4.29 (–CO–O–CH₂–), 5.57 (–C = CH₂), 6.11 (–C = CH₂), 7.66 (ArH), 8.08 (ArH). FTIR (ATR): 3500, 1714, 1473, 1262, 1243, 1097, 1016, 725 cm^{–1}.

Synthesis of bis(2-hydroxyethyl) hexane–1,6-diyl dicarbamate (1A)

1A was obtained a white powdery solid (25.68 g, 85.49% yield). Mp = 94–95°C. δ (ppm): 1.14 (m, –CH₂–), 1.28–1.30 (m, –CH₂–), 2.91–2.95 (t, –CO–NH–CH₂–), 3.58 (t, –CH₂OH), 3.94 (t, –CO–O–CH₂–).

Synthesis of 4,13-dioxo-3,14-dioxa-5,12-diazahexadecane–1,16-diyl bis(2-methylacrylate) (HDA-EC) (1B)

1B was obtained as a white powdery solid (18.80 g, 83.70% yield). Mp = 64–65°C. δ (ppm): 1.31 (m, –CH₂–), 1.46–1.50 (m, –CH₂–), 1.93 (s, –CH₃, methacrylate), 3.12–3.19 (t, –CO–NH–CH₂–), 4.30 (s, –CO–OCH₂–), 4.79 (s, –NH), 5.58 (s, –C = CH₂), 6.12 (s, –C = CH₂).

Table 1: Example formulation contains 10 wt% of a reactive diluent (50 g scale)

Polyester resin (g)	Reactive diluent (g)	Irgacure 184 (g)	Irgacure 819 (g)	Modaflow 6000 (g)	Benzoin (g)
43.00	5.00	0.75	0.75	0.375	0.125

Synthesis of bis(2-hydroxyethyl) ethane-1,2-diyl dicarbamate (2A)

2A was obtained as a white powdery solid (26.02 g, 86.79% yield). Mp = 89–92°C. δ (ppm): 3.17 (s, $-\text{CO}-\text{NH}-\text{CH}_2-$), 3.68–3.71 (t, $-\text{CH}_2\text{OH}$), 4.05–4.08 (t, $-\text{CO}-\text{O}-\text{CH}_2-$).

Synthesis of 4,9-dioxo-3,10-dioxo-5,8-diazadodecane-1,12-diyl bis(2-methacrylate) (2B)

2B was obtained as a tough, off-white solid (13.81 g, 76.76% yield). Mp = 83–86°C. δ (ppm): 1.95 (s, $-\text{CH}_3$, methacrylate), 3.32 (s, $-\text{CO}-\text{NH}-\text{CH}_2-$), 4.30–4.36 (t, $-\text{CO}-\text{O}-\text{CH}_2-$), 5.26 (s, $-\text{NH}$), 5.59 (s, $-\text{C}=\text{CH}_2$), 6.14 (s, $-\text{C}=\text{CH}_2$).

Synthesis of 2-hydroxyethyl dodecyl carbamate (3A)

3A was obtained as a white powdery solid (24.68 g, 82.99% yield). Mp = 65–66°C. δ (ppm): 0.85–0.89 (t, $-\text{CH}_3$), 1.25 (m, $-\text{CH}_2-$), 1.49–1.51 (m, $-\text{CH}_2-\text{CH}_2-\text{NH}-\text{CO}-$), 2.21 (s, $-\text{OH}$), 3.15–3.19 (t, $-\text{CO}-\text{NH}-\text{CH}_2-$), 3.79–3.82 (t, $-\text{CH}_2\text{OH}$), 4.19–4.22 (t, $-\text{CO}-\text{O}-\text{CH}_2-$), 4.77 (s, $-\text{NH}$).

Synthesis of 2-((dodecyl carbamoyl)oxy)ethyl methacrylate (DDA-EC) (3B)

3B was obtained as a white powdery solid (18.73 g, 69.27% yield). Mp = 47–51°C. δ (ppm): 0.85–0.90 (t, $-\text{CH}_3$), 1.25 (m, $-\text{CH}_2-$), 1.48–1.50 (m, $-\text{CH}_2-\text{CH}_2-\text{NH}-\text{CO}-$), 1.95 (s, $-\text{CH}_3$, methacrylate), 3.13–3.20 (t, $-\text{CO}-\text{NH}-\text{CH}_2-$), 4.31 (s, $-\text{CO}-\text{O}-\text{CH}_2-$), 4.70 (s, $-\text{NH}$), 5.58 (s, $-\text{C}=\text{CH}_2$), 6.13 (s, $-\text{C}=\text{CH}_2$).

Acid number calculations

To monitor reaction progress of the polyester syntheses, acid number calculations (according to ASTM D664) were conducted. In a typical experiment, approximately 1.00 g of the polyester was dissolved in 50 mL of CHCl_3 , along with 15 drops of phenolphthalein indicator (0.1 M in MeOH). Using a burette, 0.1 M KOH in MeOH was titrated into the polyester solution with magnetic stirring. The titration was deemed complete when a light pink color had persisted

for at least 30 s. The calculation that was used to determine acid number values is provided in equation (3):

$$TAN = \frac{56.1 \frac{\text{g}}{\text{mol}} \text{KOH} * \text{mL KOH in MeOH titrated in} * 0.1 \text{ M KOH in MeOH}}{\text{g of polyester resin}} \quad (3)$$

Powder coating formulation and application

All formulations were prepared on a 50 g scale. The MPE (96 wt%, 91 wt%, 86 wt%, or 76 wt%), the corresponding reactive diluent (0 wt%, 5 wt%, 10 wt%, or 20 wt%), photoinitiators (3 wt%; 1:1 mixture by wt. of Irgacure 184 and Irgacure 819), benzoin (degassing agent; 0.25 wt%), and Modaflow 6000 (flow modifier; 0.75 wt%) were combined in a glass jar (Table 1). Each formulation contained a fixed amount of photoinitiators, benzoin, and Modaflow 6000; only the concentration of MPE and reactive diluent was varied. This photoinitiator blend was selected based on the irradiation wavelength of the UV-lamp and previous literature studies.¹⁴ Formulations were denoted as MPE (i.e., the control with no reactive diluent) or, for example, 5_EDA-EC (5% methacrylated ethylenediamine derivative and 91% MPE base resin). Prior to extruding the formulation, the MPE was melted in a 200°C convection oven, and then cooled, to erase thermal history and ensure that the material was free of solvent. The resin was subsequently ground to a powder in a coffee bean grinder and then dry-blended with the appropriate raw materials. This was accomplished by mixing all raw materials in a pint can via shaking. Pre-mixed formulations were then fed into a Eurolab 16 mm twin screw extruder and extruded at 50 RPM between 110 and 120°C (feeder to die). The extrudate was broken into chips with a Weima granulator and then ground to a powder with a Retsch ZM 200 mill (16,000 RPM). The powder was then passed through a fine mesh sieve, using a Retsch vibratory sieve shaker, to collect particle sizes < 106 μm .

Results and discussion

As a follow-up to our previous report,¹⁹ which focused on the relationship between network formation and the thermo-mechanical properties of UV-curable polyester powder coatings that contained urethane methacrylate reactive diluents, this study evaluated how those reactive diluents influence the photopolymerization

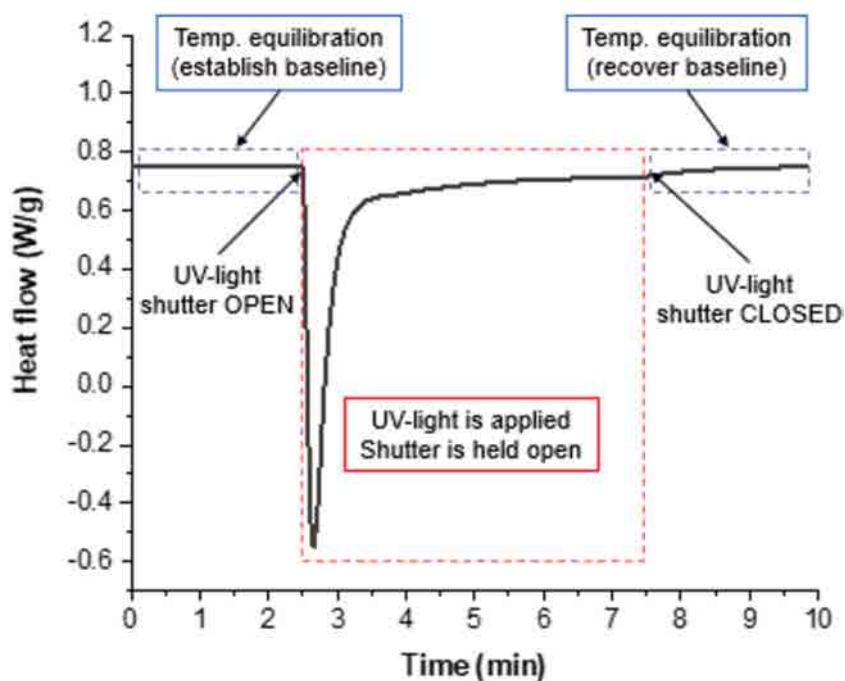


Fig. 1: Illustration of the photo-DSC experimental procedure highlighting the temperature equilibration periods and the period of UV-exposure. Total run time for each experiment was 10 min. This particular experiment (run 1 of 3) used formulation 10_DDA-EC and was conducted in a nitrogen atmosphere at 100°C, using a UV-light intensity of 1.2 mW/cm²

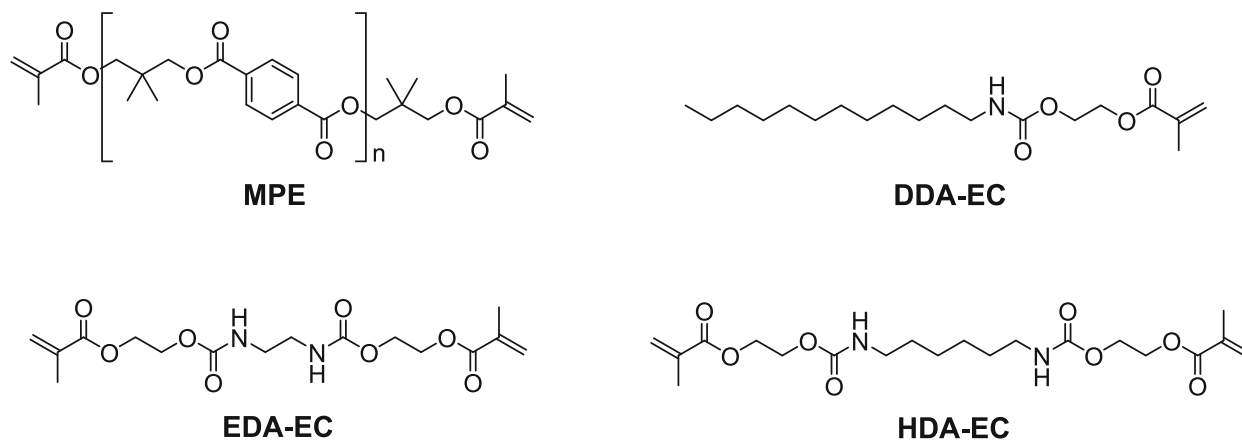


Fig. 2: Chemical structures of the methacrylated polyester oligomer and the different reactive diluents

kinetics of the system. Several variables including temperature, UV-light intensity, and air atmosphere were adjusted to understand their effects on the reaction kinetics. Cured samples were subsequently analyzed via DSC to understand how the different reaction conditions affected the T_g of the crosslinked formulations and to establish a relationship between T_g and functional group conversion.

Kinetic differences

Each of the three reactive diluents altered the photopolymerization kinetics of the formulation. The way the kinetics were affected, however, depended on the functionality and the loading level of the reactive diluent. Figure 3 displays the change in enthalpy versus time for the three different reactive diluents, at 10 wt% loading level, compared to the MPE. This information was used to determine the rate of polymerization, R_p , which can be obtained from equation (4) below, where (dH/dt) is related to the heat flow and ΔH_0 is the

enthalpy associated with complete conversion of all double bonds in the given system.¹¹ As illustrated by Fig. 3, the fastest polymerization rates were achieved with formulations that contained the di-functional reactive diluents; the slowest polymerization rates were achieved with the MPE control formulation. These trends were observed at all studied temperatures and UV-light intensities.

$$R_p = \frac{dC}{dt} = \frac{\frac{dH}{dt}}{\Delta H_{theory}} \quad (4)$$

Tables 2 and 3 report the maximum polymerization rate (R_p^{\max}) and the time it took to reach the maximum polymerization rate (tR_p^{\max}), respectively, for the different UV-curable powder coating formulations. The tR_p^{\max} is an important characteristic of UV-curable systems because it provides information on how quickly a system reaches the maximum polymerization rate. A full understanding of this attribute can help in the development of more uniform crosslinked networks with optimized material properties. The R_p^{\max} was strongly related to the reactive diluent loading level and the curing temperature that was used. The R_p^{\max} was consistently higher for the reactive diluent-containing formulations compared to the MPE control, which did not contain any reactive diluent. When the loading level of the reactive diluent was increased, a systematic increase in the R_p^{\max} was observed. For example, the R_p^{\max} of the MPE at 100°C was 0.011 s⁻¹ while the formulations that contained 5, 10, or 20 wt% HDA-EC reactive diluent had R_p^{\max} values of 0.020 s⁻¹, 0.028 s⁻¹, and 0.039 s⁻¹, respectively. The same trends were also observed when the samples were cured at lower temperatures. However, when the curing temperature was reduced, a noticeable drop of the R_p^{\max} occurred. This was particularly evident as the curing temperature was reduced from to 80°C. Figure 4 shows the R_p versus time for the 10_HDA-EC formulations when cured at 100°C, 90°C, and 80°C (left) as well as the R_p vs time for the

5_HDA-EC, 10_HDA-EC, and 20_HDA-EC formulations when cured at 90°C.

In general, the tR_p^{\max} decreased and the R_p^{\max} increased when the reactive diluents were added to the UV-curable powder coating formulations. For example, it took 20_EDA-EC 6.00 ± 0.60 s to reach its tR_p^{\max} , when polymerized at 100°C with a UV-light intensity of 1.2 mW/cm², while the MPE took 12.80 ± 0.69 s to reach its tR_p^{\max} under the same curing conditions. This corresponded to a tR_p^{\max} that was more than twice as long for the MPE compared to 20_EDA-EC. The tR_p^{\max} became even more pronounced at the lower curing temperatures. For example, it took 20_EDA-EC 8.60 ± 0.35 s to reach its tR_p^{\max} , when polymerized at 80°C with a UV-light intensity of 1.2 mW/cm², while the MPE took 51.80 ± 6.93 s to reach its tR_p^{\max} under the same curing conditions. This corresponded to a tR_p^{\max} that was more than five times as long for the MPE when compared 20_EDA-EC. Oftentimes, the reactive diluent-containing formulations had tR_p^{\max} values that were shorter than the MPE, even when the reactive diluent-containing formulation was cured at a lower temperature. Reactive diluents with unique secondary and tertiary functionalities, such as the urethane/carbamate groups, have been shown to increase the polymerization rate because of their propensity to pre-associate the reactive diluents and oligomers through hydrogen bonding interactions.^{24,25}

Effect of temperature

The reaction temperature is one of the most critical variables affecting polymerization kinetics and has been the subject of several investigations.^{11,26,27} Unlike UV-curable liquid coatings, UV-curable powder coatings require elevated temperatures to melt the sample prior to curing because of the high T_g of the amorphous resin. This makes temperature an even more critical factor for powder coatings than for liquid coatings. For amorphous powder coating resins, tem-

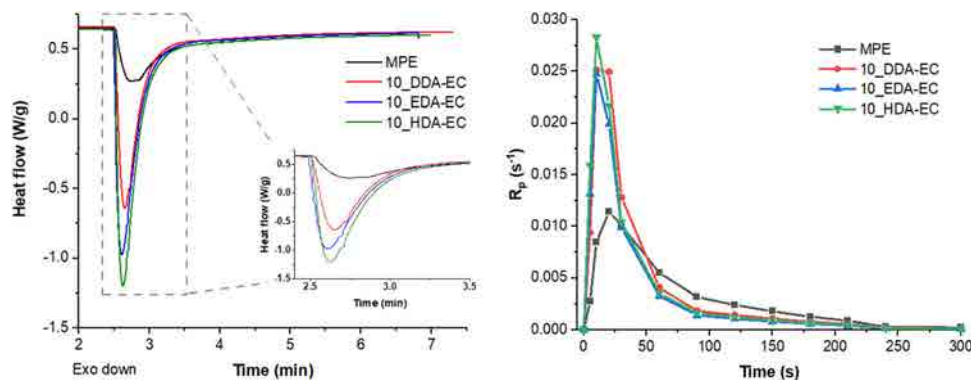


Fig. 3: Illustrates the heat flow (W/g) vs time for the MPE formulation compared against the formulations that contained 10 wt% reactive diluent (left) and the R_p vs time for the same formulations (right). The samples were polymerized in a nitrogen atmosphere, at 100°C, using a light intensity of 1.2 mW/cm²

Table 2: Comparison of the R_p^{\max} for the different UV-curable powder coating formulations when polymerized under various conditions

Formula	R_p^{\max} (s^{-1})		
	100°C, N ₂ , 1.2 mW/cm ²	90°C, N ₂ , 1.2 mW/cm ²	80°C, N ₂ , 1.2 mW/cm ²
MPE	0.011	0.007	0.002
5_DDA-EC	0.017	0.006	0.005
10_DDA-EC	0.025	0.012	0.006
20_DDA-EC	0.034	0.025	0.016
5_EDA-EC	0.019	0.010	0.006
10_EDA-EC	0.025	0.016	0.010
20_EDA-EC	0.031	0.024	0.015
5_HDA-EC	0.020	0.010	0.006
10_HDA-EC	0.028	0.017	0.010
20_HDA-EC	0.039	0.026	0.015

Table 3: Comparison of the tR_p^{\max} for the different UV-curable powder coating formulations when polymerized under various conditions

Formula	tR_p^{\max} (s)		
	100°C, N ₂ , 1.2 mW/cm ²	90°C, N ₂ , 1.2 mW/cm ²	80°C, N ₂ , 1.2 mW/cm ²
MPE	12.80 ± 0.69	20.20 ± 0.92	51.80 ± 6.93
5_DDA-EC	12.20 ± 0.92	23.80 ± 7.41	28.40 ± 2.77
10_DDA-EC	10.00 ± 1.83	14.80 ± 1.73	20.40 ± 1.04
20_DDA-EC	7.40 ± 0.69	19.00 ± 7.92	13.00 ± 0.35
5_EDA-EC	8.40 ± 0.60	14.40 ± 1.20	18.80 ± 0.35
10_EDA-EC	6.60 ± 0.60	9.80 ± 0.69	12.00 ± 0.60
20_EDA-EC	6.00 ± 0.60	7.00 ± 0.35	8.60 ± 0.35
5_HDA-EC	10.60 ± 1.51	16.40 ± 1.39	21.20 ± 1.93
10_HDA-EC	7.20 ± 1.04	11.20 ± 0.92	12.20 ± 1.25
20_HDA-EC	5.00 ± 0.35	6.80 ± 0.35	8.60 ± 0.35

peratures around the $T_g + 50^\circ\text{C}$ is most common. This translates to roughly 100–120°C. During the crosslinking process, the T_g of the polymer network will continuously increase. Eventually, the T_g will approach or even surpass the temperature at which curing takes place and vitrification of the crosslinked network will occur. Polymer chains subsequently become immobilized, which traps reactive species in the polymer matrix.^{18,28–30} Because the T_g of the network tends to increase systematically with conversion, higher curing temperatures tend to facilitate higher degrees of cure.^{11,31}

Figure 5 illustrates the kinetic behavior for the different UV-curable powder coating formulations when photopolymerized in a nitrogen atmosphere with a 1.2 mW/cm² UV-light source at either 80°C, 90°C, or 100°C. As anticipated, higher curing temperatures led

to higher degrees of conversion and faster polymerization rates (100°C > 90°C > 80°C). This was especially evident for the MPE control formulation that contained no reactive diluent. The MPE control reached a conversion of $75.52 \pm 5.61\%$ at 100°C but only $38.59 \pm 1.44\%$ at 80°C. The reactive diluent-containing samples exhibited the same behavior as the curing temperature was increased from 80 to 100°C, i.e., the photopolymerization rate and conversion increased with temperature. In most cases, the samples that were cured at 100°C had only slightly higher conversions than the same samples that were cured at 90°C. However, significantly lower conversions were obtained when the samples were cured at 80°C. Experiments were also carried out at 60°C, but the conversions were generally $\leq 10\%$ because of the high T_g of the base resin, i.e., 49°C.

As previously mentioned, a sharp decline in conversion had occurred when the curing temperature was reduced from 100 to 80°C. This was especially evident for the MPE control and the samples that contained the di-functional reactive diluents. This decline in conversion was primarily attributed to network vitrification and molecular mobility limitations. Conversely, when the mono-functional reactive diluent was used (DDA-EC), conversions of $\sim 70\%$ were achieved at 80°C. This higher extent of cure was attributed to the effect that the mono-functional reactive diluent had on viscosity, crosslink density, and the T_g . The lower formulation viscosity facilitated higher conversions because of the improved molecular mobility. The effect on T_g is important because DDA-EC does not add additional crosslinks into the polymer network like the di-functional reactive diluents do. Rather, DDA-EC reduced the overall concentration of di-functional species that were present. This reduction in crosslink density for these formulations was confirmed in our previous study via DSC and DMA experiments.¹⁹ DDA-EC also acted as an internal plasticizer because of its long alkyl side chain, which further depressed the T_g . This aliphatic tail allowed the reactive groups to have greater segmental mobility in the crosslinked network, which ultimately promoted higher degrees of cure.³² What was most surprising though was the significant increase in conversion at 80°C when just 5 wt% of the DDA-EC reactive diluent was used; 5_DDA-EC reached a conversion of $\sim 65\%$ while the MPE only reached a conversion of $\sim 39\%$.

Effect of reactive diluent loading level

The polymerization rates and the % conversion was also affected by the loading level of the reactive diluent. Figures 6 and 7 illustrate the real-time conversion plots for the mono-functional DDA-EC formulations and the di-functional EDA-EC formulations, respectively, when cured at either 80°C or 100°C. In general, increasing the concentration of the mono-functional reactive diluent led to a corresponding increase in the polymerization rate and the % conversion. This was observed for all three temperatures. However, both di-functional reactive diluents showed slightly different behavior. At 80°C and 90°C, the conversions generally increased with the loading level of the di-functional reactive diluents; at 100°C, the conversions were all roughly the same ($\pm 3\%$), regardless of the reactive diluent loading level.

Effect of UV-light intensity

Photopolymerization reactions are governed by the principles laid out in the Beer-Lambert law, i.e., the formation of initiator radicals is directly proportional to the intensity of the UV-light. As such, stronger UV-light intensities should result in faster polymerization

rates and higher degrees of conversion because more photoinitiator molecules can initiate the polymerization. Figure 8 shows the real-time conversion plot for the MPE when it was cured at 100°C with either a 1.2 mW/cm² or 12 mW/cm² UV-light intensity. As shown, both the conversion and the R_p increased when the UV-light intensity was increased. Conversion for all samples was approximately $90 \pm 3\%$, at 12 mW/cm² light intensity. Higher UV-light intensities were also used (i.e., 120 mW/cm²; un-filtered UV-light source) but the results were inconsistent due to the extremely rapid R_p . One of the disadvantages with photo-DSC is the long response time associated with the instrument.³³ Therefore, lower UV-light intensities had to be used. Nonetheless, when the T_g s of the crosslinked samples were compared, no significant difference was observed between those cured 120 mW/cm² versus those cured at 12 mW/cm². As such, because of the relationship between the T_g and % conversion for thermoset polymers, it was inferred that the samples reached a similar level of conversion, i.e., approximately 90% when cured at 100°C in the presence of nitrogen.

Effect of air atmosphere

Oxygen is a well-known and highly problematic inhibitor of free-radical polymerizations.³⁴ When oxygen interacts with free radicals that are present, unreactive peroxy radicals are formed. This inhibition process is particularly problematic at the surface layer of a film since it is directly exposed to the atmosphere. Coatings that experience significant oxygen inhibition tend to have tacky surfaces with poor appearance and diminished film properties. Stronger UV-light intensities or higher loading levels of photoinitiator are commonly used to generate a larger number of radicals. This minimizes the oxygen inhibiting effect because there is enough initiator species present to both initiate the reaction and scavenge available oxygen. Alternatively, an inert atmosphere of nitrogen, argon, or even carbon dioxide can be also used to eliminate the presence of oxygen.^{9,10,35} Unfortunately, this approach is often expensive and impractical for many large-scale applications. Other approaches such as the use of a wax barrier to prevent the diffusion of oxygen has also been used.³⁶ However, this method is also undesirable since the wax barrier can affect the physico-mechanical properties of the coating as well as the gloss. As such, the influence of breathing air on the photopolymerization kinetics of these formulations was also investigated.

Figure 9 displays the real-time conversion plots for the MPE when it was cured at 100°C, in the presence of either a nitrogen or breathing air atmosphere, using a UV-light intensity of 1.2 mW/cm². Unsurprisingly, a significant induction period was observed when the breathing air atmosphere was used. For the MPE control formulation, this induction period lasted about

1 min before the sample began to polymerize. Once the polymerization started, a slower R_p was also observed, as evidenced by the slope of the conversion vs time. This was due to the lower concentration of photoinitiator molecules present in the system since many of them had been consumed by dissolved oxygen.

Although the DSC cell was continuously supplied with breathing air throughout the course of the experiment, oxygen inhibition became less problematic once the sample started to polymerize. This was because the amount of oxygen that was diffusing into the sample had decreased as the viscosity, T_g , and crosslink density

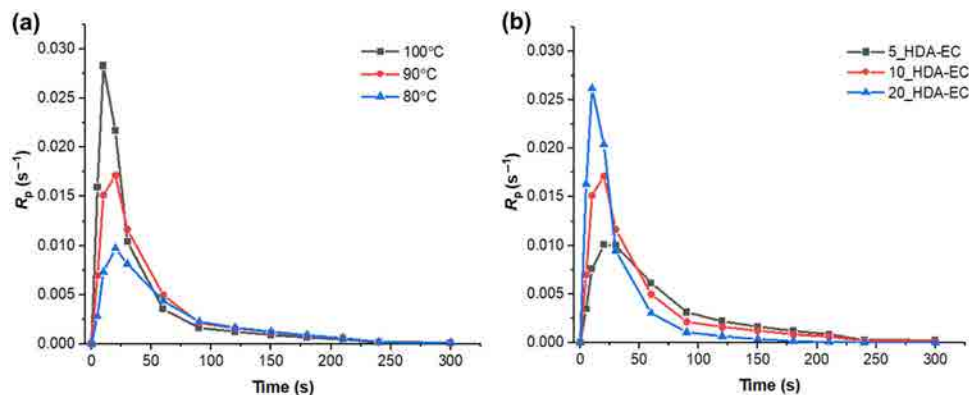


Fig. 4: (a) Illustrates the R_p vs time for the 10% HDA-EC formulations at 100°C, 90°C, and 80°C (left) as well as (b), the R_p vs time for the 5_HDA-EC, 10_HDA-EC, and 20_HDA-EC formulations when cured at 90°C (right). All examples presented above were cured in the presence of a nitrogen atmosphere using a UV-light intensity of 1.2 mW/cm^2

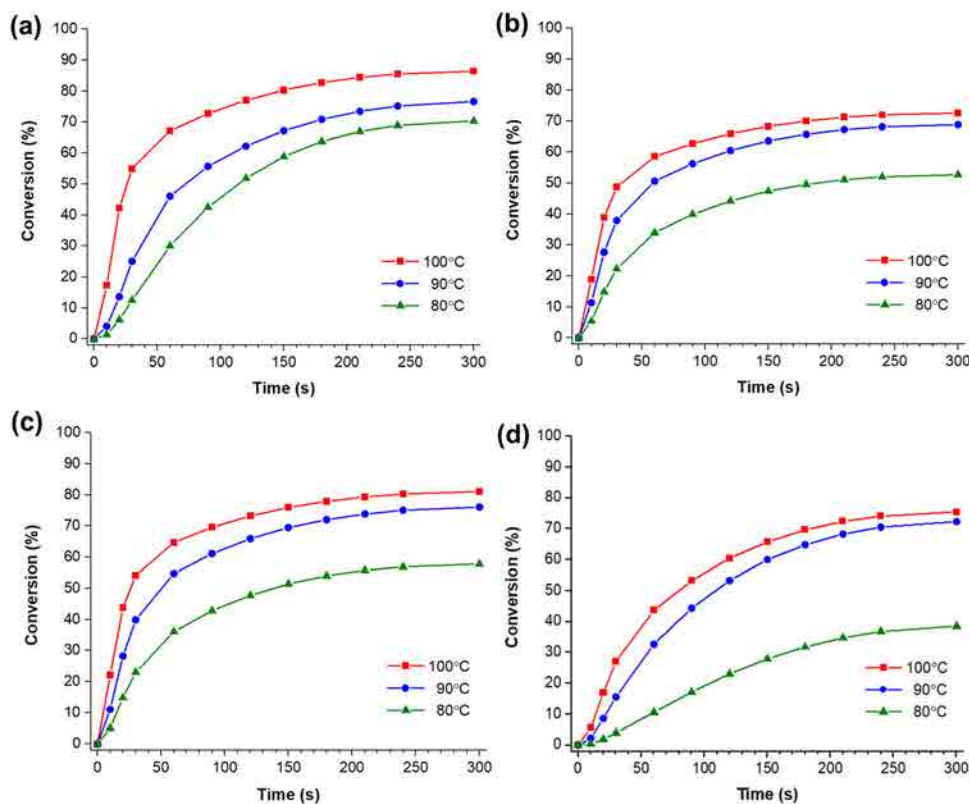


Fig. 5: Real-time conversion plots of (a) 10_DDA-EC (top left), (b) 10_EDA-EC (top right), (c) 10_HDA-EC (bottom left) and (d) MPE (bottom right) when polymerized in a nitrogen atmosphere, using a light intensity of 1.2 mW/cm^2 , and at either 100°C, 90°C, or 80°C

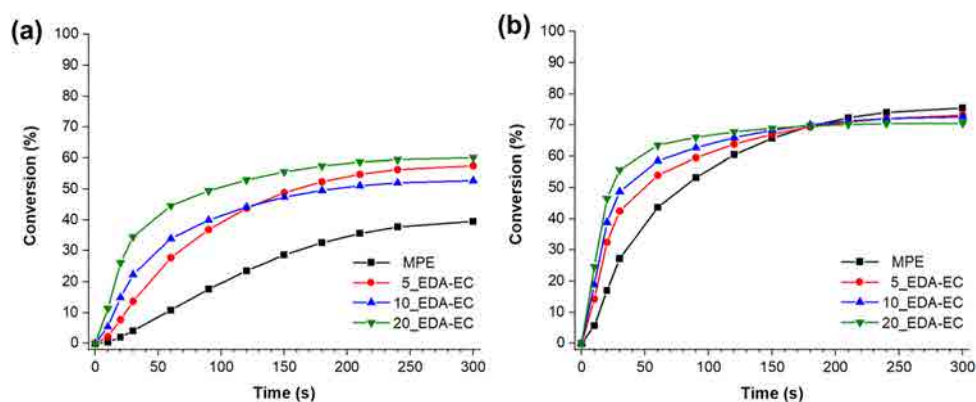


Fig. 7: Real-time conversion plots of the EDA-EC reactive diluent formulations when photopolymerized at either (a) 80°C (left) or (b) 100°C (right) in a nitrogen atmosphere, using a light intensity of 1.2 mW/cm²

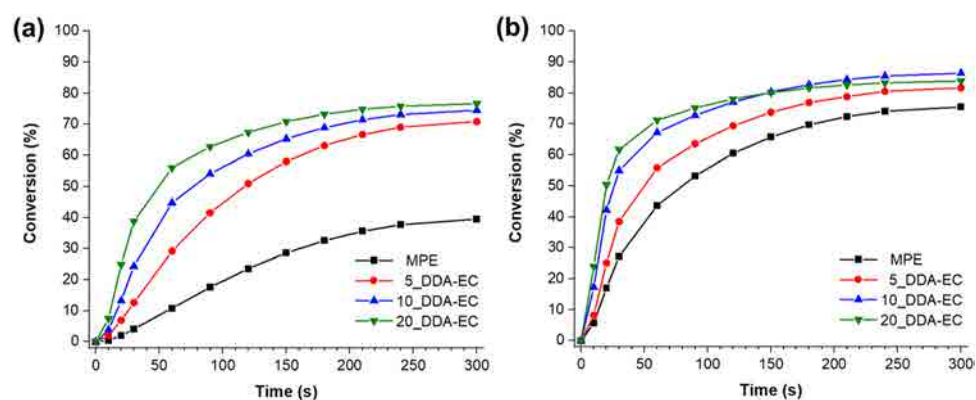


Fig. 6: Real-time conversion plots of the DDA-EC reactive diluent formulations when photopolymerized at either (a) 80°C (left) or (b) 100°C (right) in a nitrogen atmosphere, using a light intensity of 1.2 mW/cm²

increased. Similar kinetic behavior was also observed for the reactive diluent-containing formulations with comparable induction times and overall conversions. In general, the conversions of samples that were cured in the presence of breathing air ranged between ~ 40 and 50%.

Effect of curing conditions on the thermal properties

After the samples were cured in the photo-DSC, they were set aside for subsequent thermal analysis. A summary of the T_g s is provided in Table 4. As expected, each curing condition influenced the T_g of the sample. The curing temperature and the air atmosphere in which the samples were cured had the greatest impact on T_g . The highest T_g s were observed when the samples were cured at 100°C, in a nitrogen atmosphere, using a 12.0 mW/cm² UV-light source. High temperatures facilitate adequate diffusion of reactive components during the curing process due to more free volume. This is governed by the separation between the T_g of the network and the temperature at

which curing takes place ($T - T_g$). High UV-light intensities allow a greater concentration of photoinitiator molecules to be excited, thereby generating more free radicals. As such, when these two variables are optimized, the highest conversions, R_p s, and material properties can be obtained.

An upper limit appeared to exist for the T_g s of these systems. In general, the T_g s typically plateaued around $75 (\pm 5)^\circ\text{C}$. Furthermore, conversions also plateaued at $\sim 90\%$, even when stronger UV-light intensities were used. The most pronounced effect on the T_g was observed when the mono-functional reactive diluent was used. For example, 20_DDA-EC had a T_g that was 12°C lower than the MPE when cured at 100°C, in a nitrogen atmosphere, using a 1.2 mW/cm² UV-light intensity. This relatively large reduction in T_g was observed in all curing conditions for DDA-EC. This large reduction in T_g was attributed to the long flexible alkyl tail on DDA-EC, which introduced dangling chain ends into the crosslinked network. As such, this reactive diluent functioned as an internal plasticizer, which increased free volume in the crosslinked network and reduced secondary interactions such as hydrogen bonding.³⁷ Furthermore, because DDA-EC

Table 4: Summary of the T_g s, determined via DSC, for the different formulations cured under various conditions

Formula	T_g (°C)			
	100°C, N ₂ , 1.2 mW/cm ²	80°C, N ₂ , 1.2 mW/cm ²	100°C, air, 1.2 mW/cm ²	100°C, N ₂ , 12.0 mW/cm ²
MPE	71 ± 0	61 ± 1	59 ± 2	74 ± 0
5_DDA-EC	66 ± 1	59 ± 1	57 ± 1	70 ± 0
10_DDA-EC	64 ± 0	57 ± 0	51 ± 1	68 ± 1
20_DDA-EC	59 ± 1	56 ± 1	50 ± 1	64 ± 1
5_EDA-EC	69 ± 1	63 ± 1	63 ± 2	74 ± 1
10_EDA-EC	67 ± 1	63 ± 0	62 ± 1	75 ± 1
20_EDA-EC	68 ± 2	62 ± 1	64 ± 1	71 ± 2
5_HDA-EC	71 ± 0	64 ± 1	65 ± 1	78 ± 1
10_HDA-EC	68 ± 1	64 ± 2	62 ± 1	76 ± 1
20_HDA-EC	67 ± 1	65 ± 0	65 ± 1	74 ± 1

Values were rounded to the nearest whole number

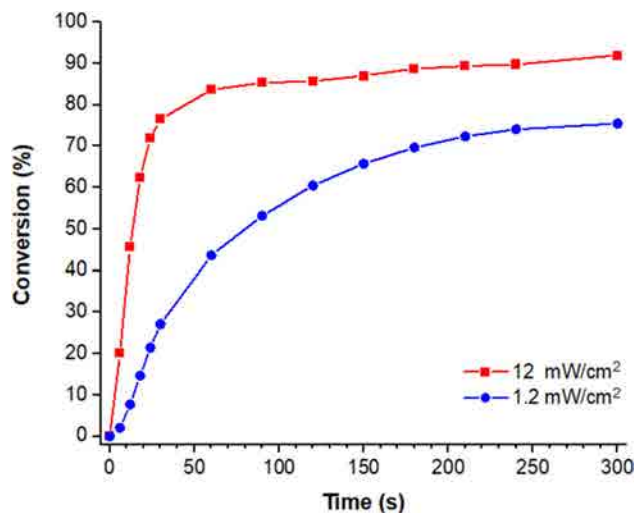


Fig. 8: Real-time conversion plot for the MPE when it was UV-cured at 100°C in a nitrogen atmosphere with either a 1.2 mW/cm² (blue) or 12 mW/cm² (red) UV-light intensity

is mono-functional, it also reduced the crosslink density of the system.

When the di-functional reactive diluents were added to the formulation, there was less of an impact on the T_g . This behavior was somewhat surprising because of the low molecular weights of the di-functional reactive diluents. In general, di-functional reactive diluents tend to increase the T_g of thermoset materials because they increase the crosslink density/reduce the molecular weight between crosslinks.³⁸ Our previous study already demonstrated that the crosslink density of these powder coating formulations increased with the loading level of the di-functional reactive diluents (via both DMA and gel-content experiments).¹⁹ However, the DMA experiments from that study showed the same trends that were observed by DSC, i.e., a negligible change in the T_g despite an increase in

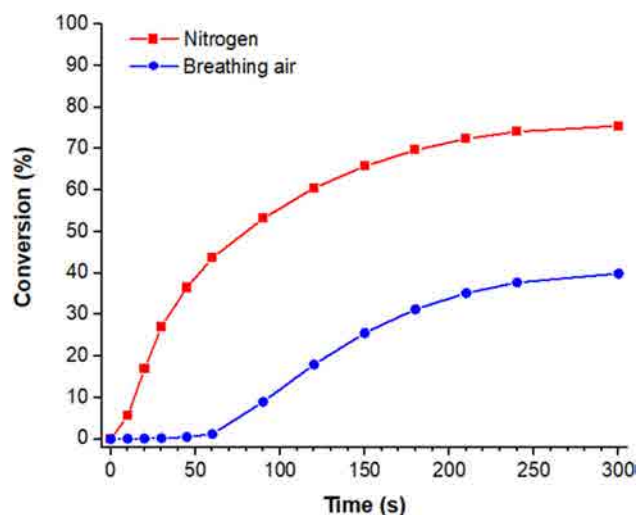


Fig. 9: Real-time conversion plot for the MPE when it was UV-cured at 100 in either the presence of nitrogen (red) or breathing air (blue). A UV-light intensity of 1.2 mW/cm² was used

crosslink density. This behavior was due to the copolymer effect. Increasing the concentration of the aliphatic di-functional reactive diluent in the formula was accompanied by a decrease in the concentration of the rigid polyester oligomer. As such, a minimal change in the T_g occurred because the di-functional reactive diluents were flexible aliphatic molecules that did not increase the rigidity of the polymeric network. Rather, these molecules had the opposite effect on the rigidity of the network, which counteracted the increase in crosslink density.

The variables that had the largest effect on the T_g were the curing temperature and the air atmosphere. The samples that were polymerized in the presence of breathing air had T_g s that were similar to the T_g s of the samples that were cured at 80°C. This was somewhat anticipated because the ultimate conversions that were

achieved with these two conditions were roughly the same, i.e., many of the samples plateaued around 50 (± 10)% conversion. However, there was one notable difference between the DSC traces for the samples that were cured at 80°C in nitrogen and those that were cured at 100°C in breathing air. Every sample that was UV-cured in the presence of breathing air showed the presence of an exotherm in the first heating scan (Fig. 10). These exotherms were attributed to the thermal scission of peroxides and hydroperoxides to form RO* and HO* radicals which, upon continued heating, resulted in additional crosslinking reactions.^{34,35}

As illustrated in Fig. 10, the samples that were polymerized in the presence of breathing air also showed the presence of two endotherms in the first heating scan. These endotherms were assigned to two T_g s, indicative of a polymer network with significant heterogeneity and phase separation.³⁰ Our previous study also identified network heterogeneity, though it was much less severe and only observed in the samples that contained high loading levels (i.e., 20 wt%) of the di-functional reactive diluents.¹⁹ The pronounced network heterogeneity identified here occurred because oxygen competed with propagation reactions and effectively halted the polymerization early on in the curing process. Since UV-curing reactions proceed by first generating microgels that subsequently grow and cluster together before reaching macrogelation,^{39–42} it is suspected that the samples that were cured in the presence of breathing air had not yet reached the macrogelation step. Therefore, the two phases correspond to crosslinked microgels that were either dominated by the reactive diluent (lower T_g) or the methacrylate-terminated oligomer (higher T_g). When the same samples were analyzed in subsequent DSC

experiments, additional crosslinking reactions took place and macrogelation of the system finally occurred. At this point, only one T_g was identified. Nonetheless, this dual T_g behavior was only observed for the samples that were polymerized in the presence of breathing air, thus highlighting the impact that a breathing air atmosphere can have on the UV-curing process.

Discussion

UV-curable powder coating technology is limited by the chemistry of its reactive oligomers. Amorphous resins with high T_g s (ca. 45–70°C) and modest molecular weights (ca. 2000–6000 g/mol) are necessary to ensure that storage stable powders can be obtained. Unfortunately, these relatively high molecular weights and T_g s also result in high melt viscosities. The high melt viscosity of UV-curable powder coating formulations counteracts the film formation process and limits the diffusion of molecular components during the curing process. As such, crosslinked films with mediocre appearance and poor degrees of conversion can be obtained with existing UV-curable powder coating systems. Therefore, a new approach that incorporated small molecule reactive diluents into the powder coating formulation was used to combat some of these issues.

Our earlier study explored how urethane methacrylate reactive diluents can be used to reduce the melt viscosity of a UV-curable polyester powder coating resin and alter the properties of the crosslinked films.¹⁹ This study evaluated how those same reactive diluents affected the photopolymerization kinetics of UV-curable polyester powder coatings. In general, adding these reactive diluents into the formulation led to a corresponding increase in both the polymerization rate and the degree of conversion. The mono-functional reactive diluent afforded the largest increase in conversion, regardless of curing temperature. In fact, many of the formulations containing the mono-functional reactive diluent that were cured at 80°C reached the same degree of conversion as the MPE control when it was cured at 100°C (i.e., about 70–75% conversion). The pronounced improvements in conversion observed for the mono-functional reactive diluent-containing formulations were driven by several variables such as the diffusion capability of the small molecule, lower formulation viscosities, and lower T_g s. The mono-functional reactive diluent was especially useful because it reduced the crosslink density and plasticized the film with its long aliphatic tail. This delayed the onset of network vitrification, which led to higher conversions. These findings suggest that the use of a mono-functional reactive diluent may permit UV-curable powder coatings to be cured at lower temperatures than what has historically been used in this field, i.e., $\sim 100^\circ\text{C}$.

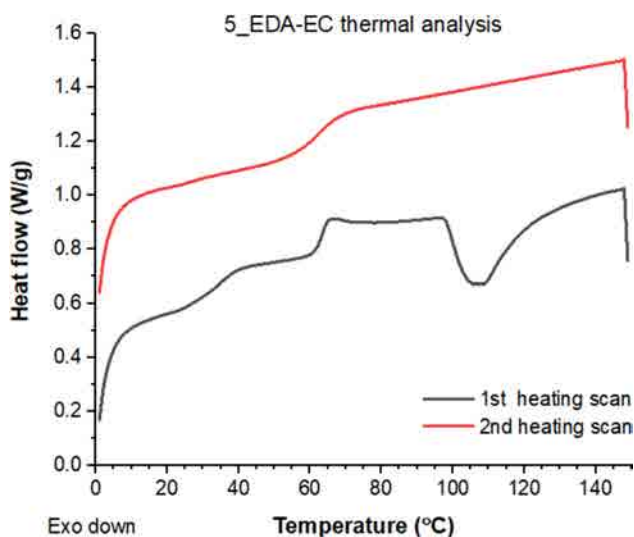


Fig. 10: DSC scans of the 5_EDA-EC sample that was UV-cured at 100°C, in the presence of breathing air, with a 1.2 mW/cm² UV-light intensity. The sample was subsequently analyzed with 20°C/min heating scans from 0 to 150°C

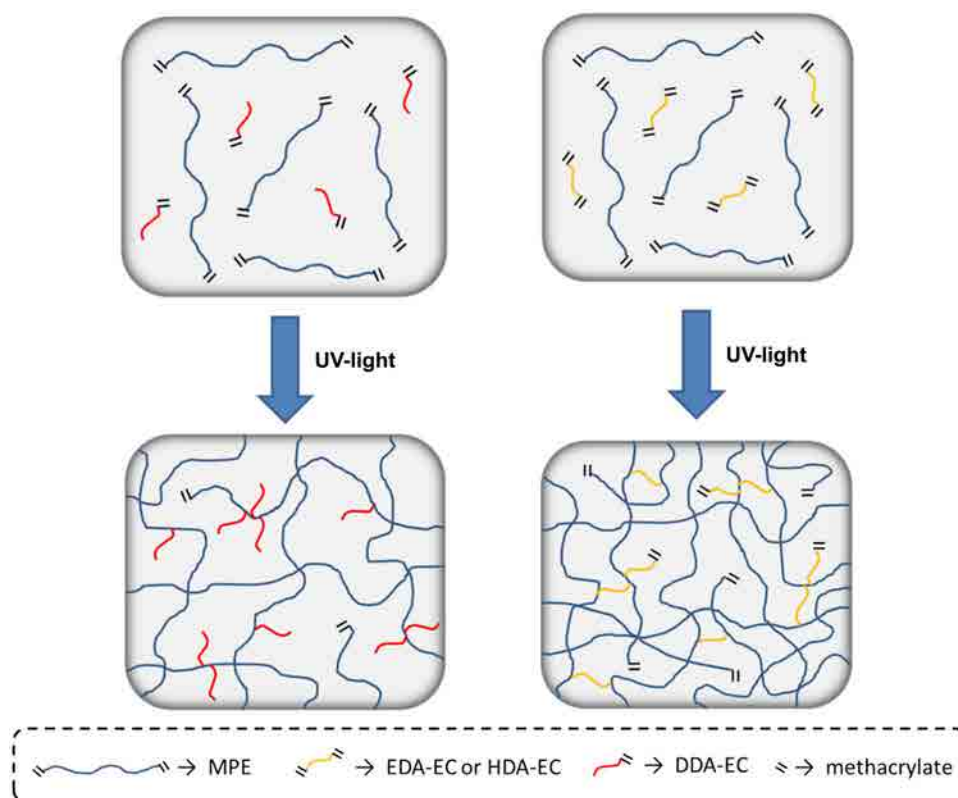


Fig. 11: Depiction of the crosslinked networks containing either the mono-functional or di-functional reactive diluents. The left side of the figure is representative of the mono-functional reactive diluent-containing network where a lightly crosslinked network with a low abundance of unreacted methacrylate groups is encountered; the right side of the figure is representative of the di-functional reactive diluent-containing networks where densely crosslinked networks with a relatively high abundance of unreacted methacrylate groups are encountered

Of the two di-functional reactive diluents that were studied, the reactive diluent with the longer methylene spacer group (HDA-EC) consistently achieved higher conversions than the reactive diluent with the shorter methylene spacer group (EDA-EC). The lower conversions that were obtained with the EDA-EC reactive diluent was likely a consequence of two factors: (1) the development of more densely crosslinked polymer networks, which limited the ultimate conversion because of vitrification; and (2) the shorter chain length of this reactive diluent, which limited its ability to diffuse through the crosslinked matrix to partake in additional crosslinking reactions. Conversely, the longer spacer group of HDA-EC facilitated higher ultimate conversions for the opposite reason, i.e., the longer chain length of HDA-EC made it more likely to encounter another photoinitiator or propagating monomer or oligomer. Regardless, both di-functional reactive diluents increased the ultimate conversion compared to the MPE control due to their viscosity reducing effect and their ability to diffuse through the crosslinking medium more effectively. Figure 11 depicts the different crosslinked networks encountered in this study when either a mono-functional (DDA-EC) or di-functional (EDA-EC or HDA-EC) reactive was

used. When the di-functional reactive diluents were used, more highly crosslinked networks were obtained. However, these networks also contained a relatively high concentration of unreacted functional (methacrylate) groups, i.e., lower conversion. Conversely, when the mono-functional reactive diluent was used, less densely crosslinked networks were obtained but these networks also contained less unreacted functional groups.

Conclusions

The photopolymerization kinetics for a series of UV-curable polyester powder coating formulations containing urethane methacrylate reactive diluents was investigated. Conversion generally increased with increasing temperature. When the formulations were cured in the presence of air, rather than nitrogen, an inhibition period was observed resulting in decreased conversion ($\leq 50\%$). This was attributed to oxygen inhibition. When the samples were cured at temperatures near the T_g of the polyester oligomer, conversion was limited due to premature network vitrification. All reactive diluent-containing formulations had higher

conversions than the MPE control due to the superior diffusion capabilities and viscosity reducing properties afforded by the reactive diluents. However, of the three reactive diluents that were studied, the mono-functional reactive diluent consistently yielded the highest conversions at all curing temperatures. This was attributed to the long alkyl side chain and mono-functionality of the reactive diluent. The side chain plasticization enhanced free volume, which resulted in lower T_g s. Additionally, because the reactive diluent only contained one functional group, it did not introduce additional crosslinks into the network, which delayed the onset of network vitrification. Ultimately, these findings suggest that incorporating mono-functional reactive diluents into UV-curable powder coating formulations can be a useful approach to increase the extent of conversion. This has the potential to create new paradigms in UV-curable powder coatings formulations that can be applied and cured at temperatures below 100°C.

Funding This work was supported by The University of Akron's School of Polymer Science and Polymer Engineering.

Conflict of interest The authors declare that they have no conflict of interest.

Open Access This article is licensed under a Creative Commons Attribution 4.0 International License, which permits use, sharing, adaptation, distribution and reproduction in any medium or format, as long as you give appropriate credit to the original author(s) and the source, provide a link to the Creative Commons licence, and indicate if changes were made. The images or other third party material in this article are included in the article's Creative Commons licence, unless indicated otherwise in a credit line to the material. If material is not included in the article's Creative Commons licence and your intended use is not permitted by statutory regulation or exceeds the permitted use, you will need to obtain permission directly from the copyright holder. To view a copy of this licence, visit <http://creativecommons.org/licenses/by/4.0/>.

References

1. MarketsandMarkets. Coating Resins Market—Global Forecast to 2025; 2020.
2. Wicks, Z, Jones, F, Pappas, P, Wicks, D, "Powder Coatings." In: *Organic Coatings: Science and Technology*, pp. 548–573. Wiley (2007)
3. Gilles de Lange, P, *Powder Coatings—Chemistry and Technology*. Vincentz Network (2004)
4. Gubbels, E, Drijfhout, JP, Posthuma-van Tent, C, Jasinska-Walc, L, Noordover, BAJ, Koning, CE, "Bio-based Semi-aromatic Polyesters for Coating Applications." *Prog. Org. Coat.*, **77** 277–284 (2014)
5. Noordover, BAJ, Heise, A, Malanowski, P, Senatore, D, Mak, M, Molhoek, L, Duchateau, R, Koning, CE, van Benthem, RATM, "Biobased Step-Growth Polymers in Powder Coating Applications." *Prog. Org. Coat.*, **65** 187–196 (2009)
6. Jones, FN, "Outlook for Zero-VOC Resins." *J. Coat. Technol.*, **73** 63–71 (2001)
7. McGinniss, V, "Ultraviolet Curable Epoxy-Polyester Powder Paints." US Patent 4,129,488, 1976
8. Udding-louwrier, S, Baijards, RA, de Jong, ES, "New Developments in Radiation-Curable Powder Coatings." *J. Coat. Technol. Res.*, **72** 71–75 (2000)
9. Studer, K, Decker, C, Beck, E, Schwalm, R, "Overcoming Oxygen Inhibition in UV-Curing of Acrylate Coatings by Carbon Dioxide Inerting, Part I." *Prog. Org. Coat.*, **48** 92–100 (2003)
10. Studer, K, Decker, C, Beck, E, Schwalm, R, "Overcoming Oxygen Inhibition in UV-Curing of Acrylate Coatings by Carbon Dioxide Inerting: Part II." *Prog. Org. Coat.*, **48** 101–111 (2003)
11. Lecamp, L, Youssef, B, Bunel, C, Lebaudy, P, "Photoinitiated Polymerization of a Dimethacrylate Oligomer: 1. Influence of Photoinitiator Concentration, Temperature and Light Intensity." *Polymer*, **38** 6089–6096 (1997)
12. Lecamp, L, Youssef, B, Bunel, C, Lebaudy, P, "Photoinitiated Polymerization of a Dimethacrylate Oligomer: 2. Kinetic Studies." *Polymer*, **40** 1403–1409 (1999)
13. Lee, TY, Guymon, CA, Jönsson, ES, Hoyle, CE, "The Effect of Monomer Structure on Oxygen Inhibition of (Meth)acrylates Photopolymerization." *Polymer*, **45** 6155–6162 (2004)
14. Castell, P, Wouters, M, Fischer, H, De With, G, "Kinetic Studies of a UV-Curable Powder Coating Using Photo-DSC, Real-Time FTIR and Rheology." *J. Coat. Technol. Res.*, **4** 411–423 (2007)
15. Cheng, XE, Huang, Z, Liu, J, Shi, W, "Synthesis and Properties of Semi-crystalline Hyperbranched Poly(esteramide) Grafted with Long Alkyl Chains Used for UV-Curable Powder Coatings." *Prog. Org. Coat.*, **59** 284–290 (2007)
16. Wei, H, Liang, H, Zou, J, Shi, W, "UV-Curable Powder Coatings Based on Dendritic Poly(ether-amide)." *J. Appl. Polym. Sci.*, **90** 287–291 (2002)
17. Maurin, V, Croutxé-barghorn, C, Allonas, X, "Photopolymerization Process of UV Powders. Characterization of Coating Properties." *Prog. Org. Coat.*, **73** 250–256 (2012)
18. Ibrahim, A, Maurin, V, Ley, C, Allonas, X, Jasinski, F, "Investigation of Termination Reactions in Free Radical Photopolymerization of UV Powder Formulations." *Eur. Polym. J.*, **48** 1475–1484 (2012)
19. Hammer, TJ, Mehr, HMS, Pugh, C, Soucek, MD, "Urethane Methacrylate Reactive Diluents for UV-Curable Polyester Powder Coatings." *J. Coat. Technol. Res.*, **18** 333–348 (2021)
20. Dickens, SH, Stansbury, JW, Choi, KM, Floyd, CJE, "Photopolymerization Kinetics of Methacrylate Dental Resins." *Macromolecules*, **36** 6043–6053 (2003)
21. Assumption, HJ, Mathias, LJ, "Photopolymerization of Urethane Dimethacrylates Synthesized via a Non-isocyanate Route." *Polymer*, **44** 5131–5136 (2003)
22. Reghunathan, H, "Photopolymerization Kinetics of Block Polyether Based Terminal Urethane Methacrylate With/Without Cross-Linker." *Adv. Polym. Technol.*, **33** 1–8 (2014)

23. Li, H, Zhang, L, Cheng, L, Kang, H, Wang, Y, "UV Curing Behavior of a Highly Branched Polycarbosilane." *J. Mater. Sci.*, **44** 970–975 (2009)
24. Berchtold, KA, Nie, J, Stansbury, JW, Hacioglu, B, Beckel, ER, Bowman, CN, "Novel Monovinyl Methacrylic Monomers Containing Secondary Functionality for Ultrarapid Polymerization: Steady-State Evaluation." *Macromolecules*, **37** 3165–3179 (2004)
25. Lu, H, Stansbury, JW, Nie, J, Berchtold, KA, Bowman, CN, "Development of Highly Reactive Mono-(meth)acrylates as Reactive Diluents for Dimethacrylate-Based Dental Resin Systems." *Biomaterials*, **26** 1329–1336 (2005)
26. Broer, DJ, Mol, GN, Challa, G, "Temperature Effects on the Kinetics of Photoinitiated Polymerization of Dimethacrylates." *Polymer*, **32** 690–695 (1991)
27. Scherzer, T, Decker, U, "The Effect of Temperature on the Kinetics of Diacrylate Photopolymerizations Studied by Real-Time FTIR Spectroscopy." *Polymer*, **41** 7681–7690 (2000)
28. Anseth, KS, Wang, CM, Bowman, CN, "Kinetic Evidence of Reaction Diffusion During the Polymerization of Multi(meth)acrylate Monomers." *Macromolecules*, **27** 650–655 (1994)
29. Nebioglu, A, Soucek, MD, "Reaction Kinetics and Microgel Particle Size Characterization of Ultraviolet-Curing Unsaturated Polyester Acrylates." *J. Polym. Sci. Part A Polym. Chem.*, **44** 6544–6557 (2006)
30. Nebioglu, A, Soucek, MD, "Microgel Formation and Thermo-Mechanical Properties of UV-Curing Unsaturated Polyester Acrylates." *J. Appl. Polym. Sci.*, **107** 2364–2374 (2007)
31. Lovell, LG, Lu, H, Elliott, JE, Stansbury, JW, Bowman, CN, "The Effect of Cure Rate on the Mechanical Properties of Dental Resins." *Dent. Mater.*, **17** 504–511 (2001)
32. Decker, C, "Kinetic Study and New Applications of UV Radiation Curing." *Macromol. Rapid Commun.*, **23** 1067–1093 (2002)
33. Cho, JD, Kim, EO, Kim, HK, Hong, JW, "An Investigation of the Surface Properties and Curing Behavior of Photocurable Cationic Films Photosensitized by Anthracene." *Polym. Test.*, **21** 781–791 (2002)
34. Pynaert, R, Buguet, J, Croutx-Barghorn, C, Moireau, P, Allonas, X, "Effect of Reactive Oxygen Species on the Kinetics of Free Radical Photopolymerization." *Polym. Chem.*, **4** 2475–2479 (2013)
35. Ligon, SC, Husa, B, Wutzel, H, Holman, R, Liska, R, "Strategies to Reduce Oxygen Inhibition in Photoinduced Polymerization." *Chem. Rev.*, **114** 557–589 (2014)
36. Bolon, DA, Webb, KK, "Barrier Coats Versus Inert Atmospheres. The Elimination of Oxygen Inhibition in Free-Radical Polymerizations." *J. Appl. Polym. Sci.*, **22** 2543–2551 (1978)
37. Gurgel, M, Vieira, A, Altenhofen, M, Oliveira, L, Beppu, MM, "Natural-Based Plasticizers and Biopolymer Films: A Review." *Eur. Polym. J.*, **47** 254–263 (2011)
38. Wang, X, Soucek, MD, "Investigation of Non-isocyanate Urethane Dimethacrylate Reactive Diluents for UV-Curable Polyurethane Coatings." *Prog. Org. Coat.*, **76** 1057–1067 (2013)
39. Dušek, K, Galina, H, Mikes, J, "Features of Network Formation in the Chain Crosslinking (Co)polymerization." *Polym. Bull.*, **25** 19–25 (1980)
40. Dušek, K, Spěváček, J, "Cyclization in Vinyl-Divinyl Copolymerization." *Polymer*, **21** 750–756 (1980)
41. Li, P, Yu, Y, Yang, X, "Effects of Initiators on the Cure Kinetics and Mechanical Properties of Vinyl Ester Resins." *J. Appl. Polym. Sci.*, **109** 2539–2545 (2008)
42. Yang, YS, Lee, LJ, "Microstructure Formation in the Cure of Unsaturated Polyester Resins." *Polymer*, **29** 1793–1800 (1988)

Publisher's Note Springer Nature remains neutral with regard to jurisdictional claims in published maps and institutional affiliations.